Accepted Manuscript

Structure-activity relationship of the inhibitory effects of flavonoids on nitric oxide production in RAW264.7 cells

Wen-Jun Jiang, Akihiro Daikonya, Mitsuyoshi Ohkawara, Takashi Nemoto, Ryusuke Noritake, Tomoko Takamiya, Susumu Kitanaka, Hiroshi Iijima

PII: S0968-0896(16)30949-X
DOI: http://dx.doi.org/10.1016/j.bmc.2016.11.055
Reference: BMC 13422

To appear in: *Bioorganic & Medicinal Chemistry*

Received Date: 13 October 2016
Revised Date: 26 November 2016
Accepted Date: 28 November 2016

Please cite this article as: Jiang, W-J., Daikonya, A., Ohkawara, M., Nemoto, T., Noritake, R., Takamiya, T., Kitanaka, S., Iijima, H., Structure-activity relationship of the inhibitory effects of flavonoids on nitric oxide production in RAW264.7 cells, *Bioorganic & Medicinal Chemistry* (2016), doi: http://dx.doi.org/10.1016/j.bmc.2016.11.055

Structure-activity relationship of the inhibitory effects of flavonoids on nitric oxide production in RAW264.7 cells

Wen-Jun Jiang, Akihiro Daikonya†, Mitsuyoshi Ohkawara, Takashi Nemoto, Ryusuke Noritake, Tomoko Takamiya, Susumu Kitanaka and Hiroshi Iijima*

School of Pharmacy, Nihon University, 7-7-1 Narashino-dai, Funabashi-shi, Chiba 274-8555, Japan

Corresponding Author

*Hiroshi Iijima. School of Pharmacy, Nihon University, 7-7-1 Narashino-dai, Funabashi-shi, Chiba 274-8555, Japan. E-mail: iijima.hiroshi@nihon-u.ac.jp. Phone/Fax: +81 47 465 6470.

Present Addresses

†Kotaro Pharmaceutical Co., Ltd., Ro 96-1, Kashima-machi, Hakusan, Ishikawa 929-0201, Japan 929-0201

Key Words

flavonoid; nitric oxide; macrophage; structure-activity relationship; comparative molecular field analysis

Abstract

We isolated flavonoids from herbal specimens from the Tibetan region (*Sophora yunnanensis* and *Rhodiola sacra*) that suppress nitric oxide (NO) production in macrophages stimulated by lipopolysaccharide and interferon-γ. The isolated flavonoids carry symmetric substitutions in the B ring ($R_{3'} = R_{5'}$). We analyzed the quantitative structure-activity relationship of the inhibitory activity by comparative molecular field analysis (CoMFA) using this series of flavonoids. Use of flavonoids with symmetrical substitutions in the B ring made it simpler to align molecules because it was not necessary to consider a huge number of combinations due to the B-ring conformation. The CoMFA model, whose cross-validated q^2 value was 0.705, suggested the existence of a hydroxy group at the 5-position, the choice of the A/C-ring scaffold (chromane or chromene) and electrostatic field around the B ring are important for NO inhibitory activity. Flavonoids synthesized based on the CoMFA model exhibited significant inhibitory potential against NO production, validating the predictive capability of the CoMFA model.

1. Introduction

Inflammation is one of important syndromes that relates to a wide range of modern diseases such as diabetes and circulatory disease. Many trials have been undertaken to identify compounds from natural resources that suppress or mitigate the progress of inflammation, especially in herbal medicine. Flavonoids are often designated as the active constituents in many traditional medicinal plants. The anti-inflammatory effects of flavonoids are explored by many *in vitro* surrogate assays such as inhibitory tests of nitric monoxide (NO) production in

macrophages, inhibitory tests of the chemotaxis of neutrophils or suppression tests on the translation of inflammation-related genes.[1-4]

Structure-activity relationship studies on the inhibitory effects of flavonoids on NO production were performed by many researchers.[5-8] However, due to the structural diversity of the flavonoids, these studies remained qualitative.

During our research into anti-inflammatory flavonoids in *Sophora yunnanensis* and *Rhodiola sacra*, we isolated the flavonoids shown in Fig. 1.[9,10] Tricin **1** and apigenin **2** are flavones (chromen-4-one scaffold). Compound **3**, laurentinol **4**, kaempferol **5** and robinetin **6** are flavonols (3-hydroxychromen-4-one scaffold). Sepinol **7**, sophorayunnanol **8**, dihydrokaempferol **9** and dihydrorobinetin **10** are flavanonols (3-hydroxychroman-4-one scaffold). Naringenin **11**, compound **12** and robitin **13** are flavanones (chroman-4-one scaffold). The B ring of these flavonoids happens to possess symmetrically arranged substituents ($R_{3'} = R_{5'}$). We determined their potential to inhibit NO production in Raw264.7 cells, a murine macrophage cell line, and intended to build a quantitative structure-activity relationship (QSAR) model.

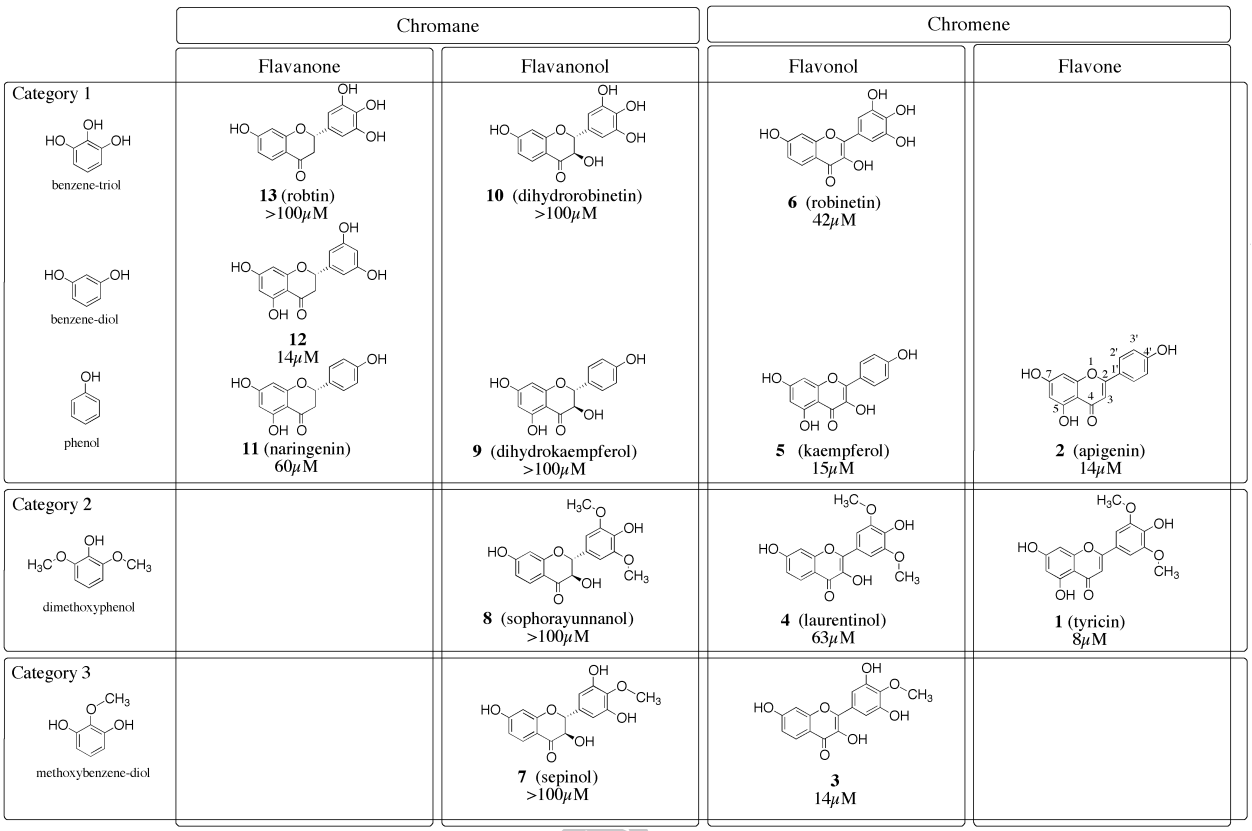

Figure 1. Structure and activity of flavonoids isolated from *Sophora yunnanensis* and *Rhodiola sacra.* Flavonoids are categorized based on the skeleton and substitution pattern of the B ring. IC_{50} values of the flavonoids for NO production in Raw246.7 cells are also indicated. Flavonoids **1**, **2**, **5**, **9**, **11** and **12** were isolated from *R. sacra*, and flavonoids **3**, **4**, **6**, **7**, **8**, **10** and **13** were isolated from *S. yunnanensis*. Atom numbering is shown in the structure of apigenin **2**. The absolute configuration of flavanonols **7**-**10** and of flavanones **11**-**13** are (2*R*, 3*R*) and (2*S*), respectively.

One reason making a structure-activity study of flavonoids difficult is the complexity caused by the conformation of the B ring. For example, as shown in Fig. 2, there are four possible combinations to overlap or align flavonoids **a** and **b**. However, if A = C and X = Z, only one alignment is available for overlapping the two flavonoids. Thus, the use of flavonoids having symmetrically substituted B rings reduces the number of possible combinations of B-ring alignments and is advantageous for 3-D structure-activity relationship studies. We conducted a comparative molecular field analysis (CoMFA) study.[11] The CoMFA model was validated by (i) predicting the activity of flavonoids of known activity reported by Matsuda *et al.*[12] and by (ii) synthesis of flavones that are expected to be active followed by evaluation of their biological activity.

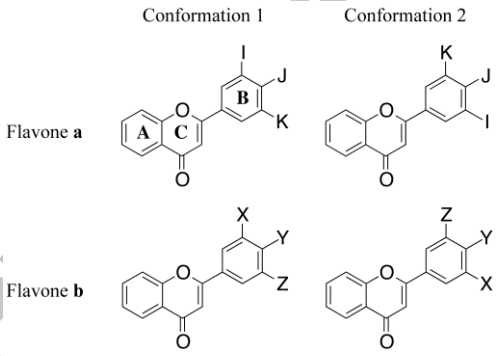

Figure 2. Symmetric B rings make alignment of molecules simpler. Provided that flavones **a** and **b** have asymmetrically substituted B rings (A ≠ C and X ≠ Z), we need to consider two conformers each from which four possible combinations arise when the flavonoid molecules are aligned (or superimposed) in space. The number of combinations grows drastically when multiple molecules are to be aligned. If both flavonoids carry symmetric B rings, such complexity is nonexistent.

2. Materials and methods

2.1 Measurement of NO Production by Macrophages *in vitro.*

Details of the assay method performed are as described previously.[9,10] In brief, RAW264.7 cells were stimulated with LPS (100 ng/mL) and IFN-γ (0.33 ng/mL). The released nitrite (NO) was quantified by the Greiss method. Cell viability was measured using AlamarBlue® reagent (Bio-Rad AbD Serotec Ltd.). The NO production inhibitory potency of the synthesized compounds **27 - 31** was tested using RAW264.7 cells stimulated by LPS only and also by LPS and IFN-γ.

2.2 Natural Flavonoids.

Flavonoids were isolated form *Sophora yunnanensis* and *Rhodiola sacra*. *S. yunnanensis* is used for the treatment of asthma, bronchitis and skin diseases. *Rhodiola* species grow in the Changbai Mountains area. The roots of *Rhodiola* have been used as a homeostasis stabilizer (adaptogen). All compounds were crystalized and were pure specimens. Details of the isolation procedure and structure determination were published elsewhere.[9,10]

2.3 CoMFA.

CoMFA available in the SYBYL-X2.0 software package[13] was used to build QSAR models. The standard procedure of CoMFA, *i.e.*, using grid space of 2 Å and the probe atom type being sp^3-carbon, was employed.

2.3.1 Outline of CoMFA Procedure.

CoMFA requires molecules to be aligned properly in space.[14] Our approach to finding such alignment was as follows. First, we built several conformational models for each of the 13 flavonoids. Then, considering possible combinations of conformers, we created 32 alignments. We submitted the 32 alignments to CoMFA and selected an alignment that gave the best partial least square evaluation, *i.e.*, a high cross-validated q^2 value and regression coefficient r^2 with a lower number of components.

2.3.2 Generation of Conformers.

The dihedral angle τ along the single bond that connects the B and the C rings (defined by atoms O1, C2, C1' and C2') is the most robust determinant of the topology of flavonoids (Fig. 3). Conformational search by using the grid search method available in the SYBYL-X was conducted, and representative energetically stable conformers were selected. The τ values of

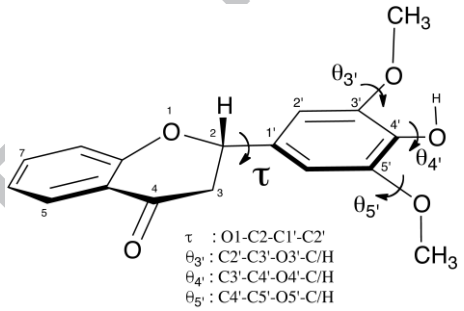

Figure 3. Definition of dihedral angles and generation of conformers. Dihedral angles that determine the conformer of flavonoids are shown. Note that these dihedral angles are not independent. For example, a conformer having ($\theta_{3'}$ = 180°, $\theta_{4'}$ = 180°, $\theta_{5'}$ = 180°) is allowed for robitin **13**, but a conformer having ($\theta_{3'}$ = 180°, $\theta_{4'}$ = 0°, $\theta_{5'}$ = 180°) would not be allowed because of unfavorable van der Waals' collision of two hydrogen atoms of the 3'- and 4'-hydroxy groups.

flavanones and flavanonols (chromane scaffold) are focused around -40°. For flavones and flavanonols (chromene scaffold), τ values of stable conformers were found around -40° and 40°. Thus, the initial dihedral angle τ was set to -40° for flavonoids bearing a chromane scaffold. For those having a chromene skeleton, two conformation models (τ = -40° and τ = 40°) were built.

The energy barrier for rotation of the C2-C1' bond is small (~5 Kcal/mol). We surveyed the distribution of the τ torsion angle values in protein-flavonoids complex structures stored in the Protein Data Bank (22 entries, 8 proteins, 11 flavonoids). As expected from the small energy barrier, the τ values distribute widely. However, in a same protein, the τ values of the ligand flavonoids focused to certain values that are specific to the host proteins. We carried out our analyses using the local minima conformations, because target proteins, if exist, on which flavonoids work to suppress NO production are unknown.

Dihedral angles of substituents on the B ring were defined as shown in Fig. 3. The dihedral angle of a hydroxy group was set to 0° or 180°. A crystallographic substructure search for 2,6-methoxyphenol moiety clearly demonstrated that the methoxy carbon atoms preferably exist in the same plane of the phenyl ring, orienting two methoxy carbon atoms apart from the oxygen atom of the central hydroxy group.[15-20] Based on this fact, for the flavonoids carrying the 4'-hydroxy-3',5'-dimethoxy substitution on the B ring (**1**, **4** and **8**), $\theta_{3'}$ and $\theta_{5'}$ were fixed at 0° and 180°, respectively. In contrast, for the flavonoids that carry the 3',5'-dihydroxy-4'methoxy phenyl ring (**3** and **7**), $\theta_{4'}$ was inevitably set to -90° or 90° to avoid unfavorable van der Waals' contact with the 3'- and 5'-hydroxy groups.

The dihedral angles of the 3-hydroxy group and 5-hydroxy group in the C and A rings were fixed to form intramolecular hydrogen bonds with a carbonyl oxygen atom at the 4 position (C2-

C3-O3-H: 180° and C4a-C5-O5-H: 0°). The dihedral angle of the 7-hydroxy group (C6-C7-O7-H) was fixed at 180°.

2.3.3 Alignment of Conformers.

The B rings of the flavonoids investigated in this study can be classified into three types: 3',4',5'-trihydroxyphenyl type (category 1), 3',5'-dimethoxy-4'hydroxyphneyl type (category 2) and 4'-methoxy-3',5'-hydroxyphenyl type (category 3) (Fig. 1 and Fig. 4). Flavonoids **6**, **10** and **13** belong to category 1. Flavanone **12** belongs to category 1 because the B ring of flavanone **12** can be recognized as a 4'-deshydroxy derivative of the category 1 framework. Similarly, the B ring of flavonoids **2, 5, 9** and **11** can be recognized as category 1, which lacks 3',5'-dihydoroxy groups. Trypsin **1**, laurentinol **4** and sophorayunnanol **8** carry the category 2 B rings whereas flavonol **3** and sepinol **7** have B rings of category 3.

The B ring of category 1 was chosen as the standard reference frame on which to superimpose B rings of the compounds. For the category 1 B ring, four conformers were premised. These four conformers were represented by an array of torsion angles of the three hydroxy groups ($\theta_{3'}$, $\theta_{4'}$, $\theta_{5'}$): *i.e.*, (0°, 0°, 0°), (0°, 0°, 180°), (0°, 180°, 180°) and (180°, 180°, 180°), as shown in Fig. 4.

Let us superimpose (or align) the B ring of laurentinol **4** (category 2) over the standard B ring having a ($\theta_{3'}$, $\theta_{4'}$, $\theta_{5'}$) = (0°, 0°, 0°) conformation. The 4'-hydroxy group of **4** was set to the same conformation of the 4'-hydroxy group of the reference ($\theta_{4'}$ = 0°). As mentioned above, the allowed torsion value for the 3'-methoxy group ($\theta_{3'}$) of **4** is 0°. ($\theta_{3'}$ = 180° is not possible because of steric collision between the methyl moiety of the 3'-methoxy group and the oxygen atom of the 4'-hyrdroxy group.) Similarly, the only available torsion angle of the 5'-methoxy ($\theta_{5'}$) of **4** is

180°. Thus, the B-ring conformation of **4** in the (0°, 0°, 180°) conformation was to be superimposed on the standard B ring in the (0°, 0°, 0°) conformation.

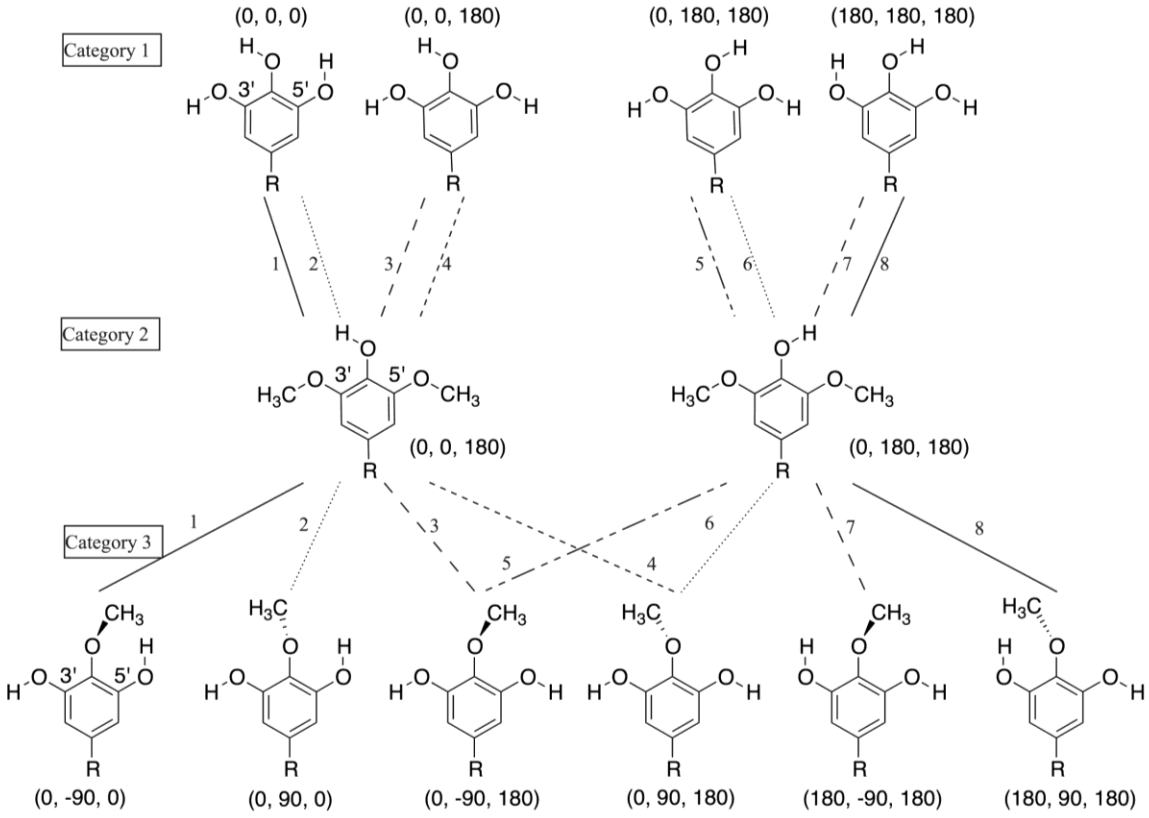

Figure 4. Combinations of B-ring conformers. Numbers indicated near the lines that link B-ring conformers represent the conformer group identification numbers.

The conformation of the B ring of category 3 that corresponds to the standard category 1 B ring in the (0°, 0°, 0°) conformation was determined as follows. The torsion angles of the 3'- and 5'- hydroxyl groups were set as those of the standard ring, *i.e.*, $\theta_{3'} = \theta_{5'} = 0°$. The methyl moiety of the 4'-methoxy group cannot be in the plane of the phenyl ring because of steric collision with

the 3'- and 5'- oxygen atoms. Thus, the torsion angle for the 4'-methoxy group of the category 3 B ring was either -90° or 90°. Two possible conformers of the category 3 B ring, (0°, -90°, 0°) and (0°, 90°, 0°), should be superimposed on the standard B ring in the (0°, 0°, 0°) conformation.

Taken together, conformers that were to be superimposed on the category 1 B ring of (0°, 0°, 0°) were (0°, 0°, 180°) for the category 2 ring and either (0°, -90°, 0°) or (0°, 90°, 0°) for the category 3 ring, leading to two possible alignments: "category 1 (0°, 0°, 0°) – category 2 (0°, 0°, 180°) – category 3 (0°, -90°, 0°)" or "category 1 (0°, 0°, 0°) – category 2 (0°, 0°, 180°) – category 3 (0°, 90°, 0°)". Such combinations are summarized in Fig. 4. Eight combinations existed.

Further, there are two possible ways to align whole structures of the 13 flavonoids. One is to align the molecules based on the A ring, and the other is to align the molecules based on the A and B rings. The former method uses six carbon atoms of the A ring and the carbonyl carbon and oxygen atoms at position 4 of the flavonoids to fit molecules. The latter uses three carbon atoms (C4' of the B ring and C5 and C7 of the A ring) to fit molecules. The former emphasizes the diversity of the B ring topology in space whereas the later maximizes the overall volume overlap of the molecules.

The two combinations of the A/C ring conformations, *i.e.* ($\tau_{chroman}$ = -40°, $\tau_{chromen}$ = -40°) and ($\tau_{chroman}$ = -40°, $\tau_{chromen}$ = 40°), eight combinations of the B-ring superimposition and the two fitting methods produced a total of 32 alignments. The torsion angles to build the initial conformers are given in supplementary data. For these 32 alignments, every conformer generated was first optimized by using the MMFF94 force field[21-25] and then by MOPAC.[26] Atomic charges of each conformer were calculated by MOPAC. Thus, the atomic charges used in this CoMFA study were conformation dependent.

The torsional angles after optimization changed from the initial values, but the deviation was small. The deviation of τ was under 15° for flavonols and flavones and under 30° for flavanones and flavanonols. Deviation values of $\theta_{3'}$, $\theta_{4'}$and $\theta_{5'}$ were under 10° for the hydroxy groups and under 30° for the methoxy groups. Thus, the molecular models were in the local minima conformations near the initial conformations.

2.4 Synthesis of 2',4',6'-Trihydroxy-2-chloroacetophenone 26.

Anhydrous $ZnCl_2$ (1.1 g, 8.0 mmol) was added to a mixture of anhydrous phloroglucinol (5.0 g, 40 mmol) and chloroacetonitrile (3.8 mL, 60 mmol) in ether (50 mL) with stirring at 0 - 5 °C (ice-water bath). When the solution was cooled to 0 - 5 °C, anhydrous HCl gas was bubbled through the reaction solution until an amount of thick yellow solid precipitated. The reaction mixture was left for 6 h. The precipitated imine was collected by filtration and washed with ether three times. The briefly dried imine was dissolved in 25 mL of distilled water. Twenty-five milliliters of aqueous 2M HCl was added to the solution and stirred for 8 h at room temperature. The precipitated solid was collected by filtration, washed three times with distilled water, and then dried under a vacuum to give **26** as a pale white powder (6.6 g, 82% yield).

^{1}H NMR (600 MHz, methanol-d_4) δ 4.91 (2H, s, H-2), 5.84 (2H, s, H-3', H-5'). ^{13}C NMR (150 MHz, methanol-d_4) δ 51.9 (C-2), 96.0 (C-3', C- 5'), 104.1 (C-1'), 165.8 (C-2', C-6'), 167.3 (C-4'), 196.7 (C-1). HR-EI-MS: *m/z* 202.0033 $[M]^+$ (Calcd 202.0033 for $C_8H_7O_4Cl$).

2.5 Synthesis of flavones

Acacetin (27).

KOH (250 mg, 4.47 mmol) ethanol solution (10 mL) was added to a solution of **26** (300 mg, 1.49 mmol) in EtOH (10 mL). Then, 4'-methoxy benzaldehyde (202 mg, 1.49 mmol) was added to the reaction mixture solution and stirred at room temperature for 3 h. Five milliliters of aqueous HCl (10 M) was added and stirred at 55 °C for 1 h. EtOH was removed under a vacuum. Distilled water was added to the residue, and the mixture was extracted with EtOAc three times. The organic layer was combined and dried over Na_2SO_4. The filtered EtOAc layer was evaporated to give a red-yellow oil that was purified by silica gel column chromatography eluting with MeOH and $CHCl_3$ to give **27** as a yellow powder (75 mg, 17.8% yield).

^{1}H NMR (600 MHz, acetone-d_6) δ 3.87 (3H, s, OCH_3-4'), 6.14 (1H, s, H-6), 6.35 (1H, s, H-8), 6.62 (1H, s, H-3), 7.04 (1H, d, J = 8.4 Hz, H-3', H-5'), 7.90 (1H, d, J = 8.4 Hz, H-2', H-6'). ^{13}C NMR (150 MHz, acetone-d_6) δ 55.9 (OCH_3-4'), 92.1 (C-8), 98.6 (C-6), 104.4 (C-10), 110.5 (C-3), 115.4 (C-3', C-5'), 126.1 (C-1'), 133.7 (C-2', C-6'), 147.7 (C-9), 158.9 (C-5), 161.8 (C-4'), 168.4 (C-7), 168.4 (C-2), 181.7 (C-4). HR-EI-MS: *m/z* 284.0683 $[M]^+$ (Calcd 284.0685 for $C_{16}H_{12}O_5$).

Diosmetin (28). KOH (250 mg, 4.47 mmol) ethanol solution (10 mL) was added to a solution of **26** (300 mg, 1.49 mmol) in EtOH (10 mL). Then, 3'-hydroxy-4'-methoxy benzaldehyde (226 mg, 1.49 mmol) was added to the reaction mixture and stirred at room temperature for 3 h. Five milliliters of aqueous HCl (10 M) was added and stirred at 55°C for 1 h. EtOH was removed under a vacuum. Distilled water was added to the residue, and the mixture was extracted with EtOAc three times. The organic layer was combined and dried over Na_2SO_4. The filtered EtOAc layer was evaporated to give a red-yellow oil that was purified by silica gel column chromatography eluting with MeOH and $CHCl_3$ to give **28** as a yellow powder (65 mg, 14.6% yield).

^{1}H NMR (600 MHz, acetone-d_6) δ 3.91 (3H, s, OCH_3-4'), 6.15 (1H, d, J = 1.8 Hz, H-6), 6.29 (1H, d, J = 1.8 Hz, H-8), 6.52 (1H, s, H-3), 7.04 (1H, d, J = 8.4 Hz, H-5'), 7.34 (1H, dd, J = 8.4, 1.8 Hz, H-6'), 7.55 (1H, d, J = 1.8 Hz, H-2'). ^{13}C NMR (150 MHz, acetone-d_6) δ 56.3 (OCH_3-4'), 91.7 (C-8), 98.8 (C-6), 104.1 (C-10), 110.1 (C-3), 112.6 (C-5'), 118.0 (C-2'), 124.7 (C-6'), 126.8 (C-1'), 147.8 (C-9), 147.8 (C-3'), 150.0 (C-4'), 159.3 (C-5), 168.7 (C-7), 168.7 (C-2), 181.0 (C-4). HR-EI-MS: *m/z* 300.0634 $[M]^+$ (Calcd 300.0634 for $C_{16}H_{12}O_6$).

4'-*O*-Methyltricetin (29). KOH (200 mg, 3.57 mmol) ethanol solution (10 mL) was added to a solution of **26** (240 mg, 1.19 mmol) in EtOH (10 mL). Then, 3',5'-dihydroxy-4'-methoxy benzaldehyde (200 mg, 1.19 mmol) was added to the reaction mixture and stirred at room temperature for 3 h. Five milliliters of aqueous HCl (10 M) was added and stirred at 55 °C for 1 h. EtOH was removed under a vacuum. Distilled water was added to the residue, and the mixture was extracted with EtOAc three times. The organic layer was combined and dried over Na_2SO_4. The filtered EtOAc layer was evaporated to give a red-yellow oil that was purified by silica gel column chromatography eluting with MeOH and $CHCl_3$ to give **29** as a yellow powder (65 mg, 17.3% yield).

^{1}H NMR (600 MHz, acetone-d_6) δ 3.87 (3H, s, OCH_3-4'), 6.15 (1H, d, J = 1.8 Hz, H-6), 6.34 (1H, d, J = 1.8 Hz, H-8), 6.46 (1H, s, H-3), 7.05 (1H, s, H-2', H-6'). ^{13}C NMR (150 MHz, acetone-d_6) δ 60.8 (OCH_3-4'), 92.1 (C-8), 98.7 (C-6), 104.2 (C-10), 110.7 (C-3), 111.6 (C-2', C-6'), 129.0 (C-1'), 138.0 (C-4'), 148.2 (C-9), 151.6 (C-3', C-5'), 158.9 (C-5), 168.5 (C-7), 168.5 (C-2), 181.7 (C-4). HR-EI-MS: *m/z* 316.0584 $[M]^+$ (Calcd 316.0583 for $C_{16}H_{12}O_7$).

3'-*O*-Methyldiosmetin (30). KOH (166 mg, 2.97 mmol) ethanol solution (10 mL) was added to a solution of **26** (200 mg, 0.99 mmol) in EtOH (10 mL). Then, 3',4'-dimethoxy benzaldehyde

(165 mg, 0.99 mmol) was added to the reaction mixture and stirred at room temperature for 3 h. Five milliliters of aqueous HCl (10 M) was added and stirred at 55 °C for 1 h. EtOH was removed under a vacuum. Distilled water was added to the residue, and the mixture was extracted with EtOAc three times. The organic layer was combined and dried over Na_2SO_4. The filtered EtOAc layer was evaporated to give a red-yellow oil that was purified by silica gel column chromatography eluting with MeOH and $CHCl_3$ to give **30** as a yellow powder (30 mg, 9.6% yield).

^{1}H NMR (600 MHz, acetone-d_6) δ 3.88 (3H, s, OCH_3-4'), 3.90 (3H, s, OCH_3-3'), 6.15 (1H, d, J = 1.8 Hz, H-6), 6.35 (1H, d, J = 1.8 Hz, H-8), 6.61 (1H, s, H-3), 7.05 (1H, d, J = 8.4 Hz, H-5'), 7.53 (1H, dd, J = 8.4, 1.8 Hz, H-6'), 7.57 (1H, d, J = 1.8 Hz, H-2'). ^{13}C NMR (150 MHz, acetone-d_6) δ 56.2 (OCH_3-3'), 56.2 (OCH_3-4'), 92.2 (C-8), 98.6 (C-6), 104.3 (C-10), 111.0 (C-3), 112.7 (C-5'), 115.1 (C-2'), 126.0 (C-6'), 126.3 (C-1'), 147.7 (C-9), 150.4 (C-3'), 151.9 (C-4'), 158.8 (C-5), 168.4 (C-7), 168.4 (C-2), 181.7 (C-4). HR-EI-MS: *m/z* 314.0791 $[M]^+$ (Calcd 314.0790 for $C_{17}H_{14}O_6$).

Apometzgerin (31). KOH (250 mg, 4.47 mmol) ethanol solution (10 mL) was added to a solution of **26** (300 mg, 1.49 mmol) in EtOH (10 mL). Then, 3',4'-dimethoxy-5'-hydroxy benzaldehyde (270 mg, 1.49 mmol) was added to the reaction mixture and stirred at room temperature for 3 h. Five milliliters of aqueous HCl (10 M) was added and stirred at 55 °C for 1 h. EtOH was removed under a vacuum. Distilled water was added to the residue, and the mixture was extracted with EtOAc three times. The organic layer was combined and dried over Na_2SO_4. The filtered EtOAc layer was evaporated to give a red-yellow oil that was purified by silica gel column chromatography eluting with MeOH and $CHCl_3$ to give **31** as a yellow powder (70 mg, 14.3% yield).

^{1}H NMR (600 MHz, acetone-d_6) δ 3.83 (3H, s, OCH_3-4'), 3.92 (3H, s, OCH_3-3'), 6.15 (1H, d, J = 1.2 Hz, H-6), 6.36 (1H, d, J = 1.2 Hz, H-8), 6.54 (1H, s, H-3), 7.10 (1H, d, J = 1.8 Hz, H-6'), 7.22 (1H, d, J = 1.8 Hz, H-2'). ^{13}C NMR (150 MHz, acetone-d_6) δ 56.4 (OCH_3-3'), 60.9 (OCH_3-4'), 92.2 (C-8), 98.7 (C-6), 104.2 (C-10), 108.2 (C-6'), 110.7 (C-3), 112.5 (C-2'), 129.1 (C-1'), 138.8 (C-4'), 148.3 (C-9), 151.5 (C-5'), 154.2 (C-3'), 158.9 (C-5), 168.5 (C-7), 168.5 (C-2), 181.6 (C-4). HR-EI-MS: *m/z* 330.0739 $[M]^+$ (Calcd 330.0740 for $C_{17}H_{14}O_7$).

3. Results and discussion

3.1 Flavonoids and Their Inhibitory Potential on NO Production.

IC_{50} values for the NO production of flavonoids isolated from *S. yunnanensis* and *R. sacra* are indicated in Fig. 1. No compound showed cell toxicity at 100 μM. Details of their isolation, structure determination and evaluation of activity were published previously.[9,10]

Flavonoids carrying a chromene scaffold tended to exhibit higher potency than those having a chromane scaffold. Flavanonols (**7 - 10**) showed poor inhibitory potency, which seemed to be related to the structure of the A/C-ring system (*i.e.*, chromane or chromene ring system). For example, the inhibitory potency of naringenin **11**, dihydrokaempferol **9**, kaempferol **5** and apigenin **2**, which commonly have a 4'-hydroxyphenyl ring as the B ring, varies widely. The existence of a hydroxy group at the 5-position tends to enhance the inhibitory potency.

3.2 CoMFA model T2c.

We ran 32 CoMFA calculations, applying the standard default conditions implemented in the SYBYL-X software package. Cross-validation was carried out using the leave-one-out procedure. The number of components was varied from 1 to 8. The inhibitory potency of the flavonoids (IC_{50} value in μM) was converted into $-\log IC_{50}$ values, which were the dependent variables. IC_{50} values higher than 100 μM were regarded as 300 μM.

		skeletone conformation					
		coplanar τ = -40°			noncoplanar τ = -40° for flavanones and flavanonols (Chromane) τ = 40° for flavones and flavonols (Chromene)		
Atoms used for alignment	B-ring confomer group #	Number of components (PLS)	Cross-validated q^2	Coreraltion r^2	Number of components (PLS)	Cross-validated q^2	Coreraltion r^2
T C5, C7 and C3' (Three atoms)	1	4	0.483	0.954	5	0.363	0.991
	2	**4**	**0.705** [a)]	**0.977**	4	0.555	0.974
	3	4	0.429	0.967	1	0.355	0.592
	4	6	0.648	0.992	5	0.594	0.988
	5	8	0.313	0.995	2	0.442	0.831
	6	6	0.519	0.983	1	0.334	0.584
	7	8	0.396	0.997	8	0.495	0.998
	8	1	0.293	0.638	1	0.378	0.609
E A-ring (C4a, C5, C6, C7, C8, C8a) , C4 and O4 (Eight atoms)	1	4	0.427	0.964	1	0.351	0.600
	2	4	0.504	0.956	2	0.446	0.850
	3	6	0.274	0.993	1	0.341	0.584
	4	8	0.522	1.000	5	0.567	0.992
	5	4	0.148	0.929	2	0.383	0.818
	6	7	0.336	0.995	2	0.341	0.810
	7	8	0.119	1.000	6	0.356	0.994
	8	4	0.223	0.944	1	0.337	0.588

Table 1. Results of CoMFA runs.

[a)] *Model T2c (Three atom alignment, group 2 type B ring combination, co-planar skeleton conforma*

From each CoMFA run, the model with the largest cross-validated q^2 (predictive coefficient) value was selected. Table 1 summarizes the characteristics of the 32 CoMFA models. Among them, model T2c had a q^2 value of 0.705 with the number of components equal to 4. The name

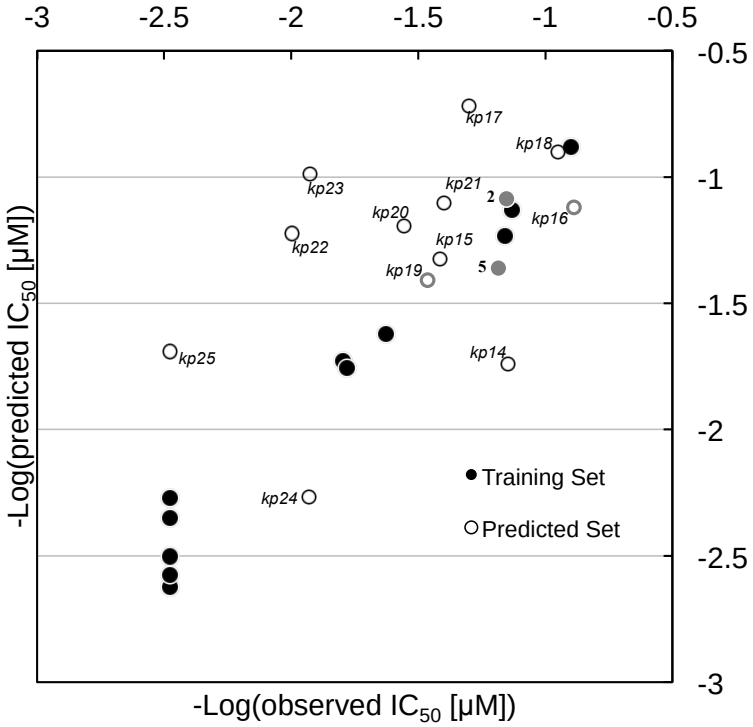

Figure 5. Regression plot of the predicted inhibitory potential (Y axis) versus the experimentally determined inhibitory potential (X axis). Closed circles indicate the experimentally determined inhibitory potential versus predicted inhibitory potential of the 13 compounds by CoMFA model T2c. Open circles indicate the inhibitory potential of flavonoids reported by Matsuda *et al.*[12] (Table 2) versus the predicted potential calculated by CoMFA model T2c (See section 3.3). Apigenin (**2**, **kp16**) and kaempeferol (**5**, **kp19**) are common compounds between our 13 compounds and those of Matsuda *et al*. Their plots are expressed using closed gray circles (our data set) and open gray circles (their data set).

T2c means that the CoMFA model was derived from conformers having a B-ring conformer group of 2 with τ value of -40° (coplanar) aligned by the three atom fitting (C5, C7 and C3'). The correlation coefficient r^2 of model T2c was 0.977 (Fig. 5, closed circles). The contribution ratios of electrostatic field and steric field were 0.56 and 0.44, respectively.

We ran CoMFA that included ClogP values as an additional variable, but no improvement was observed. Within our data set, the contribution of hydrophobicity to the inhibitory potential was not relevant.

Fig. 6-(a) depicts the CoMFA field mapping. Steric repulsive regions exist above the 2-position and below the 3-position of the C ring (regions 2 and 3). These regions indicate that the chromane scaffold is less favored for higher potency because the chromane scaffold carries hydrogen atoms at the 2- and 3-positions whereas in the chromene scaffold, the 2- and 3-positions are unsaturated, and no atom exists to interfere with the steric regions. There is a sterically favored region near the 5-position of the A ring (region 1). Flavonoids that carry a substitution at the 5-postion is advantageous for the inhibitory potency. Electrostatic mappings exist around the B ring (regions A and B). The region A is an electrostatically positive mapping and the approach of negatively charged surface of a ligand molecular is favorable for the inhibitory potency. Thus, within the scope of the 13 compounds, the inhibitory potency of flavonoids on NO production is basically explained by the electrostatic property of the B ring, the choice of the scaffold and the presence of a hydroxy group at the 5-position.

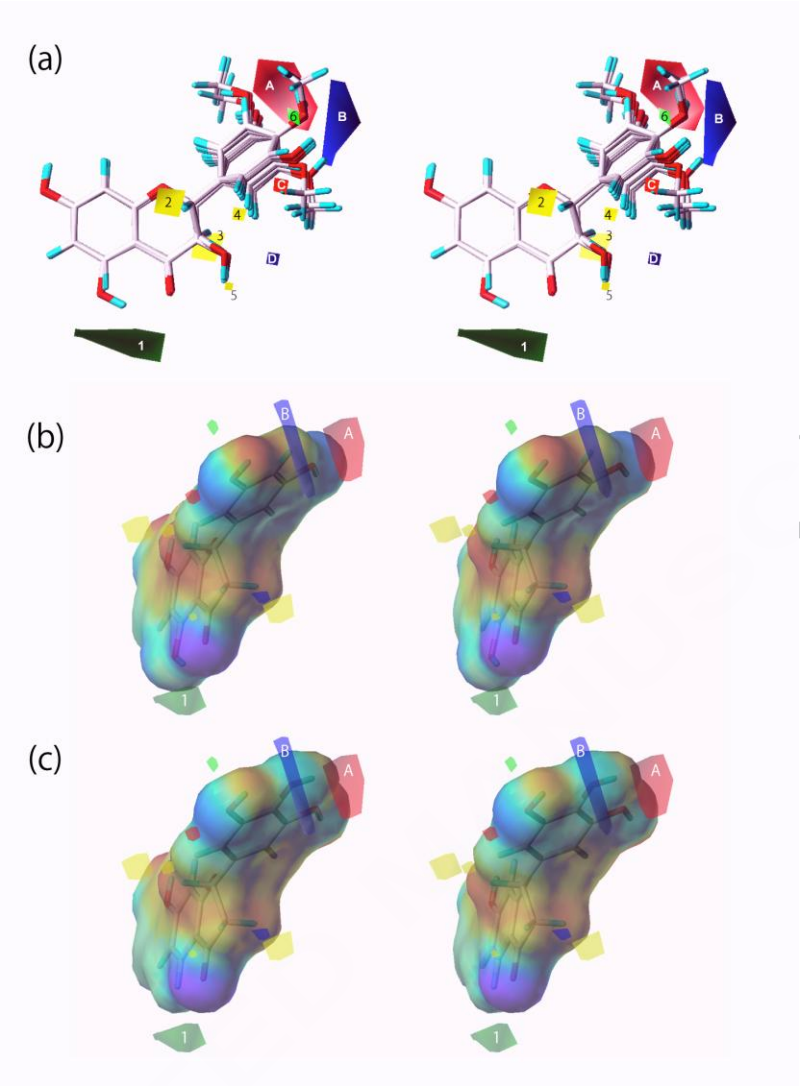

Figure 6. CoMFA field mapping of model T2c (stereo view; wall-eyes). The contours of the steric map are shown in yellow (regions 2, 3, 4, and 5) and green (regions 1 and 6), and those of the electrostatic map are shown in red (regions A and C) and blue (regions B and D). The approach of the molecular volume of a compound to the yellow region reduces the inhibitory potency whereas the existence of the molecular volume near the green region is favorable. The approach of a positive charge to the blue region is attractive and favorable, but that of a negative charge to the blue region is unfavorable. Similarly, the red region is favorable to a negative charge and unfavorable to a positive charge. (a) All 13 compounds in CoMFA mapping, (b) flavanonol **12** (high potency) and (c) flavanonol **13** (low potency) are shown.

The 13 flavanoids are shown with the CoMFA field in Fig. 6-(a). Note that the position of the B ring differs depending upon the scaffold of the A/C ring. The 3'-position of the B ring of chromenes is distant from the region A while the 3'-position of chromanes is closer to the region A. The 5'-position of chromes is closer to the region B than that of chromanes. This means that the nature of electrostatic interaction of the B rings with region A and B depends on the A/C ring systems.

Fig. 6-(b) shows flavanone **12** (IC_{50} = 12 μM) in the CoMFA mapping. The electrostatic potential was color-coded on the molecular van der Waals' surface. The electrostatic complementarity of the B ring of **12** with the region A and B are in good compatibility. Also electrostatic complementarity with region C is favorable. There also exists a favorable steric interaction between the 5-hydroxy group and the region 1. Robitin **13** is an inactive flavanone which differ from **12** in the absence of the 5-hydroxy group and in the existence of an additional hydroxy group at the 4'-position. Fig. 6-(c) shows the electrostatic potential on the molecular surface of **13** and the CoMFA mapping. The presence of the 4'-hydroxy group changes electrostatic property of the B ring into poorer complementarity with the regions A and B. Furthermore this compound lacks the 5-hydroxy substitution and interaction with the region 1 is smaller. CoMFA model suggests that the activity of flavonoids in the suppression of NO production is related to the overall topology of the molecules as well as the electrostatic property of the B ring. Indeed, flavanonol skeletons have been regarded as inactive skeletons for the inhibition of NO production, but we succeeded in synthesizing a flavanonol that exhibited an IC_{50} of 60 μM.[27]

It is unexpected that the CoMFA model T2c suggests the 4'-hydroxy group of chromanes is unfavorable for the inhibitory activity for NO production. The 4'-hydroxy group is the conserved

substitution among flavonoids because the most frequent starting unit for the biosynthesis of flavonoids is *p*-coumaric acid. Substitution of a hydroxy group or methoxy group at the 3'-position of the B ring of chromane is favorable for the inhibitory activity.

Molecular surface representations of the 13 flavonoids with the CoMFA mapping are available as supplementary data.

3.3 Validation of CoMFA model T2c: Predictive Capability.

We applied the T2c model to the structure-activity data sets complied by Matsuda *et al.*[12] Because CoMFA model T2c was derived from the 13 flavonoids with limited structural variation, it would be valid within the structural variety implemented by the 13 compounds. Thus, we selected the 12 compounds (**kp14 - kp25**, Table 2) that match the Markush structure shown in Fig. 7 from the Matsuda *et al.* data set.[12]

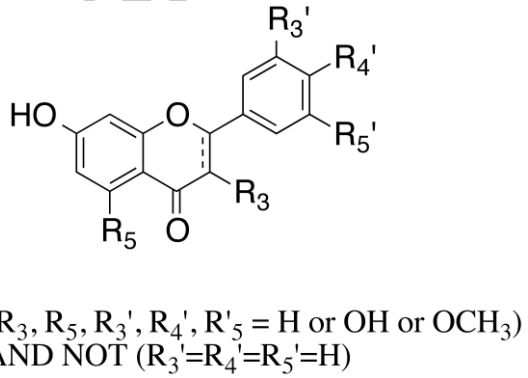

Figure 7. Markush structure used to select compounds from the original article of Matsuda *et. al.*[12] The selected compounds were predicted by CoMFA model T2c for their inhibitory potency. The correlation between predicted potency and experimental potency is plotted in Figure 5 (open circles).

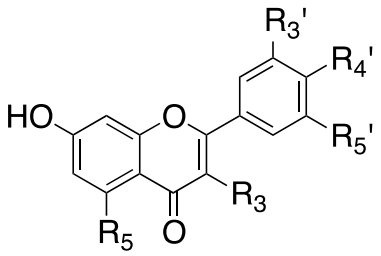

Compound		IC_{50} [μM]	R_3	R_5	$R_{3'}$	$R_{4'}$	$R_{5'}$
4',7-dihydroxyflavone	**kp14**	14	H	H	H	OH	H
3',4',7-trihydroxyflavone	**kp15**	26	H	H	OH	OH	H
Apigenin	**kp16**	7.7	H	OH	H	OH	H
Luteolin	**kp17**	20	H	OH	OH	OH	H
Diosmetin	**kp18**	8.9	H	OH	OH	OCH_3	H
Kaempferol	**kp19**	29	OH	OH	H	OH	H
Quercetin	**kp20**	36	OH	OH	OH	OH	H
Tamarixetin	**kp21**	25	OH	OH	OH	OCH_3	H
Myricetin	**kp22**	99	OH	OH	OH	OH	OH
Mearncetin	**kp23**	84	OH	OH	OH	OCH_3	OH

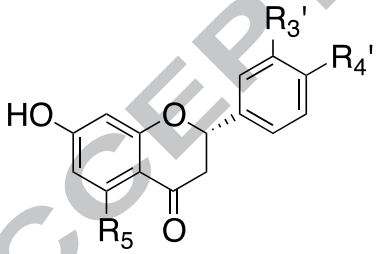

Name		IC_{50} [μM]	R_5	$R_{3'}$	$R_{4'}$
Liquiritigenin	**kp24**	85	H	H	OH
Eriodictyol	**kp25**	> 100	OH	OH	OH

Table 2. Structure-activity data from Matsuda *et.al.* [12]

It should be noted that the assay methods of Matsuda *et al.* were not identical to ours. They determined the inhibitory potency of flavonoids on NO production using peritoneal exudate cells collected from the peritoneal cavity of ddY mice, and they stimulated the cells only by LPS.[12] We tested the 13 compounds using RAW264.7 cells, a murine macrophage cell line, and we stimulated the cells with LPS (100 ng/mL) and IFN-γ (0.33 ng/mL). The method used to quantify NO production was the same (Greiss method[10,12]).

Two compounds were commonly included in the Matsuda *et al.* data set and in ours. The IC_{50} value of apigenin **2** was 14 μM in our evaluation and was reported to be 8 μM in theirs (**kp16**), and that of kaempeferol **5** was 15 μM in our evaluation and 29 μM in theirs (**kp19**). Given that these divergences are permissible, we applied the T2c model to predict the potency of the Matsuda *et al.* compounds. For the compounds carrying asymmetrically substituted B rings, two possible B ring orientations were evaluated, and the one with the lower IC_{50} value (more potent activity) was chosen. In Fig. 5, the experimental IC_{50} values and the predicted values of the Matsuda *et al.* compounds were plotted, and a reasonable predictive ability of the CoMFA model T2c was shown. Prediction of the inhibitory activity of compounds having high lipophilicity (**kp14** and **kp24**) tended to be lower than the observed activity and that of the compounds with lower lipophilicity (**kp17**, **kp22**, **kp23** and **kp25**) was overestimated. This fact suggests that cell permeability of the compounds or their perturbation into the cell membrane might be relevant. Indeed, no glycosylated flavonoid is known to inhibit NO production. We have observed that the inhibitory activity of NO production in RAW264.7 cells of flavanonols is stereospecific, and flavanonols having (2*R*, 3*R*) stereochemistry are active but the (2*S*, 3*S*) enantiomers are not.[27] Taken together, flavonoids would interact with certain target molecule(s) that stereochemically recognizes flavonoid molecules. Many previous studies reported that the NO inhibitory function

of flavonoids is associated with the suppression of inducible nitric oxide synthase (*i*NOS) biosynthesis.[7,12]

3.4 Validation of CoMFA Model T2c: Synthesis of Active Compounds.

We constructed a virtual compound library, which was composed of chromen-4-ones that carry a phenyl having 3'-, 4'- and 5'-substitutions (Fig. 8). The inhibitory potency of the virtual compounds was predicted by the model T2c. Of the predicted activity of the virtual compounds having asymmetrical substitutions in the B-ring, the one indicating a lower IC_{50} value was chosen. In general, compounds having a 3,5-dihydroxyflavone skeleton were predicted to indicate higher inhibitory potential, and the compounds having a 3'-methoxy substitution in the B ring were predicted to be preferable for their high potency. Detail of the virtual library and the predicted IC_{50} values by the model T2c is available as supplementary data.

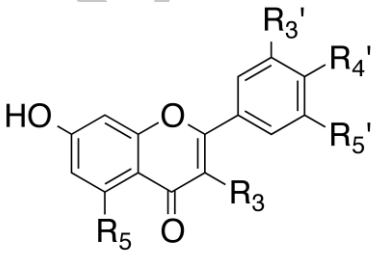

R_3= H or OH

R_5=O or OH

R_3', R_4', R_5' = H or OH or OCH_3

Figure 8. Structures of virtual compounds. Virtual compounds defined by this Markush structures were modeled and their inhibitory potency was predicted by CoMFA model T2c. Five compounds were selected and synthesized. Their inhibitory potency is shown in Table 3.

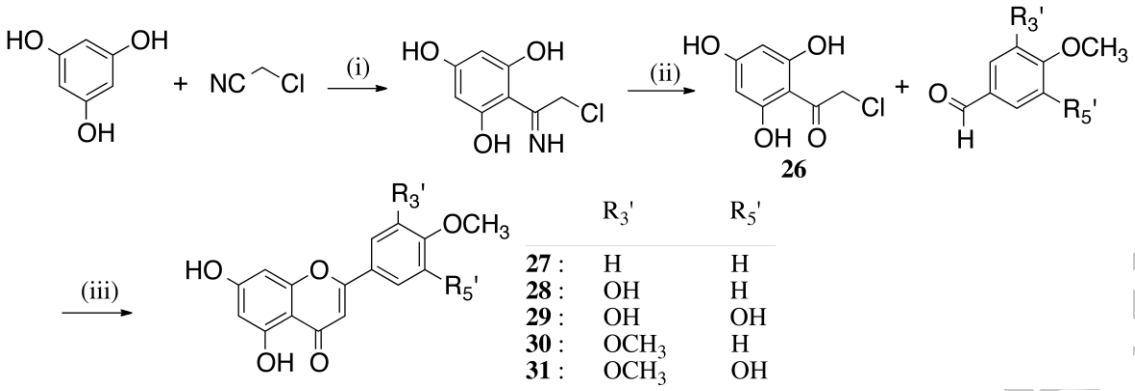

Scheme 1. Synthesis of flavones. Reagents and conditions: (i) (1) $ZnCl_2$, Et_2O (2) HCl gas, 0-5 °C; (ii) 1 M HCl aqueous, rt; (iii) (1) KOH, EtOH, rt; (2) HCl aqueous, 55 °C.

Five flavones, **27** - **31**, that were predicted to be potent by the model T2c were synthesized as shown in Scheme 1. An intermediate, 2',4',6'-trihydroxy-2-chloroacetophenone **26,** was prepared by the hydrolysis of 2-(2-chloro-1-iminoethyl)benzene-1,3,5-triol, which was synthesized from phloroglucinol and chloroacetonitrile aided by $ZnCl_2$. Benzaldehyde derivatives were reacted with **26** to yield flavones **27** - **31**.

The inhibitory potency for NO production of compounds **27** - **31** is summarized in Table 3. We carried out two types of assay. One is our conventional assay in which RAW264.7 cells are stimulated by LPS and IFN-γ, and the other is similar to the Matsuda *et al.* method whereby the cells are stimulated only by LPS. Compound **28** is diosmetin, and its IC_{50} was 16.7 μM (LPS)/32.2 μM (LPS/IFN-γ). This compound was included in the Matsuda *et al.* data set as **kp18** (Table 2). Its IC_{50} was reported as 8.9 μM (LPS) and was the third most potent flavonoid in their data set. Compounds **30** (3'-*O*-methyldiosmetin) and **31** (apometzgerin) showed higher potency

than **28** in our assay: IC_{50} 5.0 μM (LPS)/17.0 μM (LPS/IFN-γ) and 6.9 μM (LPS)/18.2 μM (LPS/IFN-γ), respectively. It seemed that the existence of the 3'-methoxy group on the B ring was important for the inhibitory activity of 5,7-dihydroxy-flavanones. Actually, tricine **1** has an IC_{50} value of 8 μM (LSP/IFN-γ) as shown in Fig. 1. IC_{50} values of compounds **27** and **29** were 27.7 μM (LPS)/53.7 μM (LPS/IFN-γ) and 37.0 μM (LPS)/59.3 μM (LPS/IFN-γ), respectively. Compounds **27 - 31** did not show cell toxicity at 100 μM.

Unfortunately, the diversity of the A/C ring was very small in our data set. It is interesting that Matsuda *et al.* reported that 3',4',5,7-tetramethoxy-flavone (tetra-*O*-methyl-luteolin) showed the highest inhibitory potential among the 73 compounds they investigated.[12] Considering that 3',4',5,7-tetramethoxy-flavone is very hydrophobic, hydrophobicity might be important for its

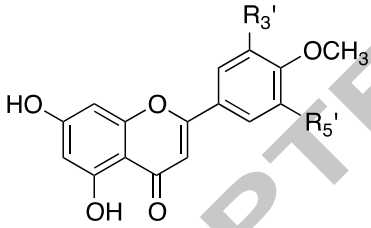

Compound		$R_{3'}$	$R_{5'}$	LPS only		LPS + INF-γ	
				NO production-inhibitory IC_{50} (μM)	Cell viability (%)	NO production-inhibitory IC_{50} (μM)	Cell viability (%)
Acacetin	**27**	H	H	27.7±0.1	99±2	53.7±3.2	115±11
Diosmetine	**28**	OH	H	16.7±1.7	108±6	32.2±1.9	109±6
4'-*O*-Methyltricetin	**29**	OH	OH	37.0±1.9	112±6	59.3±4.5	119±9
3'-*O*-Methyldiosmetin	**30**	OCH_3	H	5.0±0.5	112±5	17.0±2.9	109±6
Apometzgerin	**31**	OCH_3	OH	6.9±0.4	106±6	18.2±1.3	96±2
Control (AG)				33.7±1.1	105±1	78.3±1.6	102±3
Kaempferol				13.4±0.5	141±3	17.0±2.0	138±7

Table 3. NO production-inhibitory activity of the designed compounds

activity. We are currently undertaking a synthetic study of flavonoids to further expand structural diversity and hydrophobicity with the aim to more fully establish the structure-activity relationship of flavonoids on their inhibitory potency against NO production.

4. Conclusion

We carried out a CoMFA study on the inhibitory activity of flavonoids against NO production. We constructed the possible alignments of 13 flavonoids systematically. For this process, the use of symmetrically substituted analogues was the key to reducing the possible numbers of alignments to a feasible size. The CoMFA model T2c reasonably explained the structure-activity relationship. The preference of the chromene scaffold over the chromane scaffold was expressed as sterically unfavorable regions above the 2-position and below the 3-position. The preference for the existence of a hydroxy group at the 5-position was expressed as a sterically favorable region between the 4- and 5- positions. The CoMFA fields around the B ring are mostly electrostatic fields, suggesting that electrostatic features of the B-ring substitutions are important. Because the topology of the B ring alters depending on the scaffold, the effects of the B-ring substitutions on inhibitory potency would differ scaffold by scaffold, and this rendered CoMFA a robust methodology in this study. The CoMFA model T2c exhibited a predictable capability, and this model rationally helped us to obtain very potent compounds **30** and **31**. To our knowledge, their inhibitory potential against NO production has not been reported so far, and this study appears to be the first to report the inhibitory potency of these compounds.

Abbreviations

CoMFA, comparative molecular field analysis; IFN-γ, interferon-γ; LPS, lipopolysaccharide; NO, nitric oxide

Acknowledgement

Part of this study was supported by the Academic Frontier Project of the Ministry of Education, Culture, Sports, Science and Technology. We thank the Otsuka Toshimi Scholarship Foundation and Watanuki International Scholarship Foundation for supporting the study and research of author W.-J.J. We thank Dr. Masateru Ohta (Chugai Pharmaceutical Co., Ltd.) for discussions and insightful suggestions.

References

1. Santana, F. P. R.; Pinheiro, N. M.; Mernak, M. I. B.; Righetti, R. F.; Martins, M. A.; Lago, J. H. G.; dos Santos Lopes, F. D. T. Q.; Tibério, I. F. L. C.; Prado, C. M. *Mediators Inflamm*. **2016**, 2348968.

2. Leyva-López, N.; Gutierrez-Grijalva, E. P.; Ambriz-Perez, D. L.; Heredia, J. B. *Int. J. Mol. Sci.* **2016**, *17*, 921.

3. Devia, K. P.; Malara, D. S.; Nabavib, S. F.; Suredac, A.; Xiaod, J.; Nabavib, S. M.; Dagliaf, M. *Pharmacol. Res*. **2015**, *99*, 1.

4. Chirumbolo, S. *Inflamm. Allergy Drug Targets*. **2010**, *9*, 263.

5. Jnawali, H. N.; Lee, E.; Jeong, K-W.; Shin, A.; Heo, Y-S.; Kim, Y. *J. Nat. Prod.* **2014**, *77*, 258.

6. Lyu, S. Y.; Park, W. B. *Arch. Pharm. Res*. **2005**, *28*, 573.

7. Kim, A. R.; Cho, J. Y.; Zou, Y.; Choi, J. S.; Chung, H, Y. *Arch. Pharm. Res.* **2005**, *28*, 297.

8. Kim, S. J.; Park, H.; Kim, H. P. *Arch. Pharm. Res.* **2004**, *27*, 937.

9. Daikonya, A.; Kitanaka, S. *Chem. Pharm. Bull.* **2011**, *59*, 1567.

10. Daikonya, A.; Kitanaka, S. *Japanese Journal of Food Chemistry and Safety*. **2011**, *18*, 183.

11. Cramer III, R. D.; Patterson, D. E.; Bunce, J. D. *J. Amer. Chem. Soc.* **1988**, *110*, 5959.

12. Matsuda, H.; Morikawa, T.; Ando, S.; Toguchida, I.; Yoshikawa, M. *Bioorg. Med. Chem.* **2003**, *11*, 1995.

13. SYBYL-X 2.0 (2013), Certara USA. Inc., 100 Overlook Center, Suite 101, Princeton, NJ 08540 USA.

14. Kubinyi, H.; Hamprecht, F.A.; Mietzner, T. *J. Med. Chem.* **1998**, *41*, 2553.

15. Thipparaboina, R.; Mittapalli, S.; Thatikonda, S.; Nangia, A.; Naidu, V. G. M.; Shastri, N. R. *Cryst. Growth Des.* **2016**, *16*, 4679.

16. Lai, Y.; Liu, T.; Sa, R.; Wei, X.; Xue, Y.; Wu, Z.; Luo, Z.; Xiang, M.; Zhang, Y.; Yao, G. *J. Nat. Prod.* **2015**, *78*, 1740.

17. Sinha, A. S.; Rao Khandavilli, U. B.; O'Connor, E. L.; Deadman, B. J.; Maguire, A. R.; Lawrence, S. E. *Cryst. Eng. Comm.* **2015**, *17*, 4832.

18. Xie, T.; Liu, Z.; Liu, Q.; *J. Struct. Biol.* **2015**, *190*, 155.

19. Tominaga, M.; Kunitomi, N.; Katagiri, K.; Itoh, T. *Org. Lett.* **2015**, *17*, 786.

20. Sallum, L. O.; Napolitano, H. B.; Carvalho, Pde. S. Jr.; Cidade, A. F.; de Aquino, G. L.; Coutinho, N. D.; Camargo, A. J.; Ellena, J.; de Oliveira, H. C.; Silva, V. H. *J. Phys. Chem. A.* **2014**, *118*, 10048.

21. Halgren, T. A. *J. Comp. Chem.* **1996**, *17*, 490.

22. Halgren, T. *J. Comp. Chem.* **1996**, *17*, 520.

23. Halgren, T. A. *J. Comp. Chem.* **1996**, *17*, 553.

24. Halgren, T. A. *J. Comp. Chem.* **1996**, *17*, 587.

25. Halgren, T. A. *J. Comp. Chem.* **1996**, *17*, 616.

26. Quantum Chemistry Program Exchange #455. Indiana University, Bloomington, IN 47405, USA.

27. Jiang, W.-J.; Ishiuchi, K.; Furukawa, M.; Takamiya, T.; Kitanaka, S.; Iijima, H. *Bioorg. Med. Chem.* **2015**, *23*, 6922.

Figure Legends

Fig. 1. Structure and activity of flavonoids isolated from *Sophora yunnanensis* and *Rhodiola sacra*. Flavonoids are categorized based on the skeleton and substitution pattern of the B ring. IC_{50} values of the flavonoids for NO production in Raw246.7 cells are also indicated. Flavonoids **1**, **2**, **5**, **9**, **11** and **12** were isolated from *R. sacra*, and flavonoids **3**, **4**, **6**, **7**, **8**, **10** and **13** were isolated from *S. yunnanensis*. Atom numbering is shown in the structure of apigenin **2**. The absolute configuration of flavanonols **7**-**10** and of flavanones **11**-**13** are (2*R*, 3*R*) and (2*S*), respectively.

Fig. 2. Symmetric B rings make alignment of molecules simpler. Provided that flavones **a** and **b** have asymmetrically substituted B rings (A ≠C and X ≠Z), we need to consider two conformers each from which four possible combinations arise when the flavonoid molecules are aligned (or superimposed) in space. The number of combinations grows drastically when multiple molecules are to be aligned. If both flavonoids carry symmetric B rings, such complexity is nonexistent.

Fig. 3. Definition of dihedral angles and generation of conformers. Dihedral angles that determine the conformer of flavonoids are shown. Note that these dihedral angles are not independent. For example, a conformer having ($\theta_{3'}$ = 180°, $\theta_{4'}$ = 180°, $\theta_{5'}$ = 180°) is allowed for robitin **13**, but a conformer having ($\theta_{3'}$ = 180°, $\theta_{4'}$ = 0°, $\theta_{5'}$ = 180°) would not be allowed because of unfavorable van der Waals' collision of two hydrogen atoms of the 3'- and 4'-hydroxy groups.

Fig. 4. Combinations of B-ring conformers. Numbers indicated near the lines that link B-ring conformers represent the conformer group identification numbers.

Fig. 5. Regression plot of the predicted inhibitory potential (Y axis) versus the experimentally determined inhibitory potential (X axis). Closed circles indicate the experimentally determined inhibitory potential versus predicted inhibitory potential of the 13 compounds by CoMFA model T2c. Open circles indicate the inhibitory potential of flavonoids reported by Matsuda *et al.*[12] (Table 2) versus the predicted potential calculated by CoMFA model T2c. Apigenin (**2**, **kp16**) and kaempeferol (**5**, **kp19**) are common compounds between our 13 compounds and those of Matsuda *et al*. Their plots are expressed using closed gray circles (our data set) and open gray circles (their data set).

Fig. 6. CoMFA field mapping of model T2c (stereo view; wall-eyes). The contours of the steric map are shown in yellow (regions 2, 3, 4, and 5) and green (regions 1 and 6), and those of the electrostatic map are shown in red (regions A and C) and blue (regions B and D). The approach of the molecular volume of a compound to the yellow region reduces the inhibitory potency whereas the existence of the molecular volume near the green region is favorable. The approach of a positive charge to the blue region is attractive and favorable, but that of a negative charge to the blue region is unfavorable. Similarly, the red region is favorable to a negative charge and unfavorable to a positive charge. (a) All 13 compounds in CoMFA mapping, (b) flavanonol **12** (high potency) and (c) flavanonol **13** (low potency) are shown.

Fig. 7. Markush structure used to select compounds from the original article of Matsuda *et. al.*[12] The selected compounds were predicted by CoMFA model T2c for their inhibitory potency. The correlation between predicted potency and experimental potency is plotted in Fig. 5 (open circles).

Fig. 8. Structures of virtual compounds. Virtual compounds defined by this Markush structures were modeled and their inhibitory potency was predicted by CoMFA model T2c. Five compounds were selected and synthesized. Their inhibitory potency is shown in Table 3.

Scheme 1. Synthesis of flavones. Reagents and conditions: (i) (1) $ZnCl_2$, Et_2O (2) HCl gas, 0-5 °C; (ii) 1 M HCl aqueous, rt; (iii) (1) KOH, EtOH, rt; (2) HCl aqueous, 55 °C.

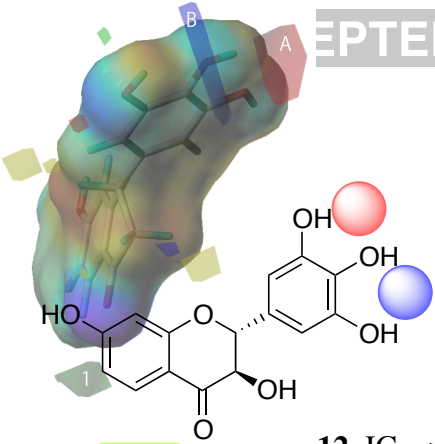

12 $IC_{50} > 100\mu M$

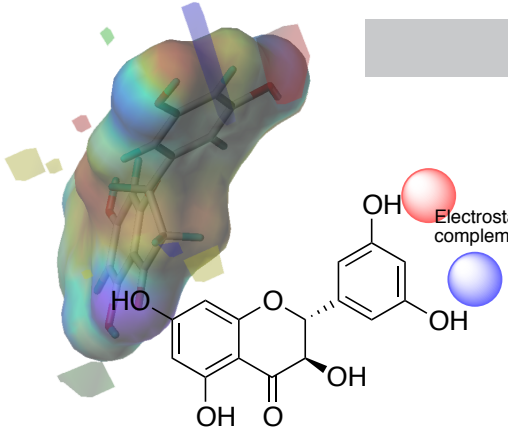

13 $IC_{50} = 14\mu M$